Deel I

Two-Field Inflation

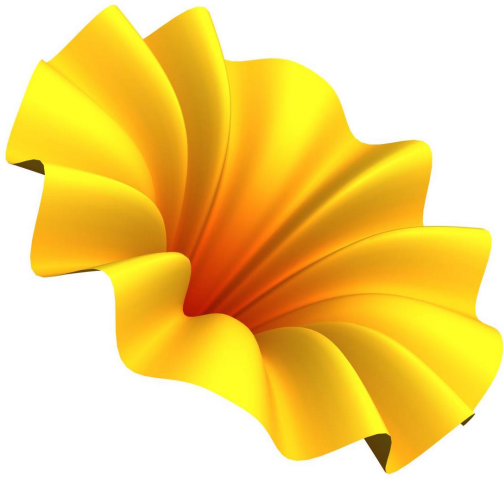

Orbital Inflation

The purpose of this chapter is two-fold. First of all, it serves as a short introduction to multi-field inflation. Second, we introduce Orbital Inflation as one of the simplest way to extend the single field scenario.

We start with a brief recap of the linear perturbation analysis of multi-field inflation in § 2.2. If we consider more than one field, the comoving curvature perturbation interacts with *isocurvature perturbations* (quanta of the other fields). It turns out that the linear dynamics of multi-field inflation can be described in terms of a few kinematical and geometrical parameters. In case of two-field inflation, these are the field *radius of curvature*, the effective mass of isocurvature perturbations (*entropy mass*) and the Hubble slow-roll parameters. This motivates us to introduce Orbital Inflation: a family of two-field models of inflation where all these parameters are (approximately) constant. We discuss their phenomenology in § 2.3. Finally, by means of the Hamilton-Jacobi formalism we locally reconstruct potentials in § 2.4 that admit Orbital Inflation. This allows us to numerically test our predictions.

2.1 Introduction

What can we learn about inflation from the density perturbations that we observe in the sky? In case inflation is driven by a single light degree of freedom, the observational data can be described in terms of the Hubble slow roll parameters, the sound speed of the curvature perturbation, and its self-couplings. This suggests we should classify inflationary models by the behavior of these parameters, rather than by their potential. Essentially, this is what the effective field theory of single field inflation [162] does. If another light degree of freedom is active during inflation, we additionally may hope to infer its mass, its coupling to the inflaton and its self-interactions [192].

We eventually hope to come closer to the understanding of what drives inflation. Therefore, it is important to give the parameters that describe the data an interpretation in terms of the essential features of the UV embedding

of inflation. For instance, the data coefficients may inform us about the presence of extra dimensions or interactions with other fields with a certain spin, see e.g. [193–195] For that reason, it is important to understand how various classes of inflationary theories affect the low energy dynamics of the curvature perturbation, possibly coupled to other light degrees of freedom.

In the context of multi-field inflation, the observational parameters are understood to be of kinematical and geometrical origin. In particular, in two-field inflation the dynamics of the inflaton coupled to the isocurvature perturbations are, to linear order, described in terms of the *radius of curvature* of the inflationary trajectory, the mass of the isocurvature perturbation (*entropy mass*) and the Hubble slow-roll parameters. This motivates us to introduce *Orbital Inflation*: a family of models in which the inflationary trajectory has a constant radius of curvature. Moreover, we take the entropy mass to be approximately constant. From the observational point of view, this is the simplest set-up to consider beyond single field.

Orbital Inflation is an attempt to realize 'spontaneous symmetry probing' [196] in the context of inflation. Moreover, it provides a realisation of quasi-single field inflation [100, 101]. We complement these studies in the following ways:

- We focus on the phenomenology in the regime of small entropy mass and relatively small radius of curvature. In particular, we allow the coupling strength to become much larger than typically considered in quasi-single field inflation (while staying in the perturbative regime.) Two results we would like to emphasize are:
  - The entropy mass dictates how the predictions for n_s change. For a decreasing radius of curvature, the value of r gets reduced. However, the shift in n_s depends on the value of the entropy mass. The predictions for (n_s, r) shift downwards and fan-out. This may help to distinguish the value of the entropy mass.
  - The larger the coupling to the isocurvature perturbations, the more they become suppressed relative to the curvature perturbations [138]. We discuss how the ratio of the power spectra at the end of inflation depends on both the entropy mass and the radius of curvature.
- We *locally* reconstruct potentials which provide exactly the kinematical properties of orbital inflation by means of a generalization of the Hamilton-Jacobi formalism [74, 75, 77, 78]. This reconstruction method

allows us to test our analytical predictions numerically. Moreover, this reconstruction method provides a playground for any quasi-single field model of inflation [100, 101] or spiral inflation [197], for which, to our knowlegde, no exact models are known. Higher order couplings can be tuned as well. Interestingly, a vanishing entropy mass is reflected by a shift symmetry in the Hubble parameter rather than the resulting potential.

In this chapter we briefly review the kinematical analysis of multi-field inflation in § 2.2. This allows us to describe the phenomenology of Orbital Inflation in § 2.3. Finally, we show how to contruct exact models of Orbital Inflation in § 2.4.

Throughout this chapter we work in Planck units $\hbar = c = 1$ and the reduced Planck mass is given by $M_p = (8\pi G)^{-1/2}$.

2.2 Kinematical analysis of multi-field inflation

In § 1.2 we have seen that the observable predictions of the simplest models of inflation[1] are, besides an overall energy scale, fully characterized by the kinematical Hubble slow-roll parameters

$$\epsilon \equiv -\frac{\dot{H}}{H^2}, \quad \epsilon_{n+1} \equiv \frac{\dot{\epsilon}_n}{H\epsilon_n} \quad \text{for} \quad n \geq 2. \tag{2.1}$$

Here it is understood that $\epsilon = \epsilon_1$ and moreover, we will denote $\eta = \epsilon_2$ and $\xi = \epsilon_3$. To second order in perturbation theory we can characterize the data by means of power spectra and bispectra of the scalar and tensor perturbations. Canonical single field inflation predicts

$$r = 16\epsilon, \quad n_s = 1 - 2\epsilon - 2\eta, \quad n_t = -2\epsilon, \quad f_{NL}^{\text{sq, obs}} = 0\ . \tag{2.2}$$

Here r is the tensor-to-scalar ratio, n_s and n_t are the spectral indices of the scalar and tensor power spectrum respectively and $f_{NL}^{\text{sq, obs}}$ is the observable [109] amplitude of the bispectrum in the squeezed limit. For conciseness we don't show other predictions, such as the amplitude of scalar perturbations and the amplitude of the bispectrum in other configurations. Importantly, if we

[1] With the simplest models of inflation we mean canonical single-field slow-roll inflationary models minimally coupled to gravity, and with Bunch Davies initial conditions.

were to detect a violation of the single field consistency relation [81, 105, 109] $f_{NL}^{\text{sq, obs}} = 0$, this would signal the presence of additional degrees of freedom.

To understand how the inflationary predictions Eq. 2.2 are affected if more degrees of freedom are active during inflation, we turn to the kinematical analysis of multi-field inflation, following the formalism developed in [198–201] (see also [202–204] and [205] for a comparative study). We identify the relevant kinematical parameters that characterise the dynamics of perturbations. For simplicity we restrict ourselves to linear perturbation theory. We start by assuming some general structure, namely minimal coupling to Einstein gravity, a field space, and as scalar field potential. In other words, we study models of multi-field inflation of the general form

$$S = \frac{1}{2}\int d^4x\sqrt{-g}\left[M_p^2 R - G_{ab}\partial_\mu\phi^a\partial^\mu\phi^b - 2V(\phi^a)\right] . \tag{2.3}$$

Here G_{ab} is the field metric characterizing the kinetic terms. Moreover, R is the Ricci scalar of spacetime and $V(\phi^a)$ the potential energy density of the scalar fields. Our aim is to eventually arrive at the perturbation equations in terms of kinematical quantities only. Furthermore, one also expects the appearance of geometrical parameters that characterise the field space.

2.2.1 Background dynamics

The background dynamics of the scalar fields follows from assuming a homogeneous, isotropic and flat Friedmann Lemaitre Robertson Walker spacetime $ds^2 = -dt^2 + a^2(t)d\mathbf{x}^2$. The field equations and Friedmann equations are given by [198]

$$D_t^2\phi^a + 3HD_t\phi^a + V^a = 0, \tag{2.4a}$$

$$3H^2M_p^2 = \frac{1}{2}G_{ab}\dot\phi^a\dot\phi^b + V(\phi^a), \tag{2.4b}$$

$$\dot H M_p^2 = \frac{1}{2}G_{ab}\dot\phi^a\dot\phi^b, \tag{2.4c}$$

respectively, where $D_t \equiv \dot\phi^a\nabla_a$, with ∇_a the covariant field derivative with respect to the field metric. Moreover, the latin field indices are raised and lowered with the field metric. The last equation is not independent from the first two, but nevertheless useful later, when we construct exact models of Orbital Inflation in § 3.3.

Kinematical basis in field space

The inflationary background trajectory determines a natural basis of unit vectors in field space [199, 201, 206], which are defined iteratively[2]:

$$T^a = \frac{\dot{\phi}^a}{\dot{\varphi}}, \tag{2.5a}$$

$$D_t T^a = -\Omega N^a, \tag{2.5b}$$

$$D_t N_j^a = \Omega_j N_{j-1}^a - \Omega_{j+1} N_{j+1}^a \quad \text{for } j \geq 1 \quad \text{with} \quad N_i^a (N_i)_a = 1 \quad \forall\, i\ . \tag{2.5c}$$

Please see Figure 2.1 for an illustration. The first vector T^a is the tangent pointing along the inflationary trajectory. The other ones are the normal vectors, which are all normalized to unity. This uniquely determines the values of the turn rates Ω_i up to a sign. Furthermore, it is understood that $N_0^a = T^a$, $N^a = N_1^a$ and $\Omega = \Omega_1$. Finally, $\dot{\varphi} \equiv \sqrt{G_{ab}\dot{\phi}^a\dot{\phi}^b}$ is the *proper field velocity*.

In § 2.3 and § 2.4 we will work with the field *radius of curvature* of the inflationary trajectory

$$\kappa \equiv \dot{\varphi}\,(N_a D_t T^a)^{-1}\ . \tag{2.6}$$

Notice that this is related to the turn rate as $\kappa = -\frac{\sqrt{2\epsilon}M_p H}{\Omega}$.

Geodesics and turns

Using the tangent vector instead of $\dot{\phi}^a$, the field equations of motion can be written as

$$D_t T^a + \frac{V^a - V_T T^a}{\dot{\varphi}} = 0\ . \tag{2.7}$$

This shows explicitly that the field trajectory is a geodesic only if $V^a = V_T T^a$, because in that case the tangent vector T^a is parallel transported, i.e. $D_t T^a \sim T^b \nabla_b T^a = 0$. Moreover, the deviation of a geodesic is parameterized by the turn rate Ω defined above. If we consider only two fields, we may choose N^a to have a fixed orientation with respect to the tangent vector, namely $N^a = \epsilon^{ab} T_b$. Then Ω will flip sign each time the inflationary trajectory changes from turning clockwise to anti-clockwise or vice versa. In the multi-field scenario it is perhaps more convenient to assign a definite sign to all Ω_i.

[2] This procedure becomes ill-defined as soon as a turn rate Ω_i becomes zero. In that case we can choose the remaining normal vectors N_n^a, for $n \geq i$, as any orthogonal normal set of vectors (and $\Omega_n = 0$).

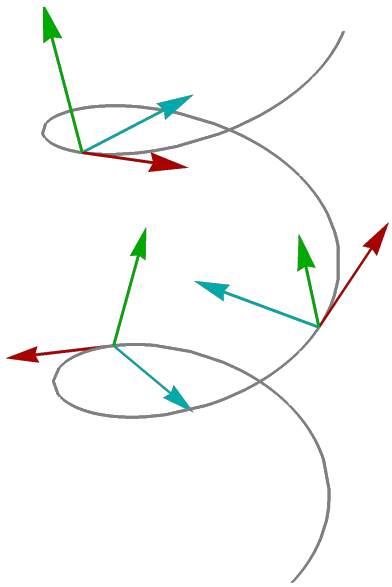

Figuur 2.1: Illustration of an inflationary trajectory in a three-dimensional field space and the corresponding tangent (red), normal (cyan) and binormal (green) vector. In this example the inflationary trajectory is along a helix, and both turn rates Ω_1 and Ω_2 are non-zero.

Tangent and normal projections of the field equations

Projecting the equations of motion along the kinematical basis vectors we find

$$\ddot{\varphi} + 3H\dot{\varphi} + V_T = 0, \tag{2.8a}$$
$$V_N = \Omega\dot{\varphi}, \tag{2.8b}$$
$$V_{N_i} = 0 \quad \text{for } i > 1. \tag{2.8c}$$

This is an alternative way of writing the field equations Eq. 2.4a. The first equation is the same as in single field inflation, and it suggests we should identify φ with the inflaton field. The remaining projections express a condition on the gradient of the potential to sustain centrifugal motion.

Kinematical expression for the gradient of the potential

The background equations allow us to write the gradient of the potential in terms of the slow roll parameters and the first turn rate. The Hubble slow roll parameters are defined in Eq. 2.1. Using Eq. 2.4, the first three slow-roll parameters can be written as

$$\epsilon \equiv -\frac{\dot{H}}{H^2} = \frac{\dot{\varphi}^2}{2H^2 M_p^2}, \tag{2.9a}$$

$$\eta \equiv \frac{\dot{\epsilon}}{\epsilon H} = \frac{2\ddot{\varphi}}{\dot{\varphi}H} + 2\epsilon, \tag{2.9b}$$

$$\xi \equiv \frac{\dot{\eta}}{\eta H}. \tag{2.9c}$$

The projections of the background equations Eq. 2.8 therefore imply the following kinematical expression for the potential gradient

$$V_a = -\dot{\varphi}H(3 - \epsilon + \tfrac{1}{2}\eta)T_a + \Omega\dot{\varphi}N_a \ . \tag{2.10}$$

2.2.2 Linear perturbations

Perturbing around the homogeneous background, the linearized equations of motion of field perturbations are given by [201, 207–210]

$$\frac{D^2}{dN^2}Q^a + (3-\epsilon)\frac{D}{dN}Q^a + \frac{k^2}{a^2H^2}Q^a + C^a{}_b Q^b = 0, \tag{2.11a}$$

$$\text{with} \quad C^a{}_b \equiv \frac{\nabla_b V^a}{H^2} - 2\epsilon M_p^2 R^a{}_{cdb} T^c T^d + 2\epsilon(3-\epsilon)T^a T_b + \frac{2\epsilon}{\varphi' H^2}\left(T^a V_b + T_b V^a\right) \ . \tag{2.11b}$$

The covariant derivatives are with respect to efolds $\frac{D}{dN} \equiv H D_t$. Moreover, Q^a are the gauge invariant field fluctuations.

These equations can be rewritten in terms of the *comoving curvature perturbation* $\mathcal{R} \equiv \frac{HT_a Q^a}{\dot{\varphi}}$ and *isocurvature perturbations* $\mathcal{S}_i \equiv \frac{(N_i)_a Q^a}{M_p}$ [202] by projecting Eq. 2.11 along the kinematical basis vectors Eq. 2.5. Since for the rest of this chapter we specialize to the two-field scenario, we only quote the corresponding two field equations

$$\left(\frac{\partial}{\partial_N} + 3 - \epsilon - \eta\right)\left(\mathcal{R}' + \frac{2\Omega}{\sqrt{2\epsilon}H}\mathcal{S}\right) + \frac{k^2}{a^2H^2}\mathcal{R} = 0, \tag{2.12a}$$

$$\left(\frac{\partial}{\partial_N} + 3 - \epsilon\right)\mathcal{S}' - \frac{2\Omega\varphi'}{H}\left(\mathcal{R}' + \frac{2\Omega}{\sqrt{2\epsilon}H}\mathcal{S}\right) + \left(\frac{\mu^2}{H^2} + \frac{k^2}{a^2H^2}\right)\mathcal{S} = 0 \ . \tag{2.12b}$$

Here a prime denotes a derivative with respect to efolds and $S \equiv S_1$. The perturbations are grouped in such a way that we can read off the *entropy mass* (the effective mass of the first isocurvature mode) most easily. The entropy mass is given by

$$\mu^2 \equiv V_{NN} + 2\epsilon H^2 M_p^2 R_{NTNT} + 3\Omega^2, \tag{2.13}$$

Here we use the notation $V_{NN} \equiv N^a N^b \nabla_a \nabla_b V$ and $R_{NTNT} \equiv N_a T^b N^c T^d R^a{}_{cdb}$. We explain in § 2.2.3 by means of a dispersion relation analysis why this is the correct interpretation of the mass of isocurvature perturbations.

2.2.3 Dispersion relation analysis

To understand why we interpret μ^2 (defined in Eq. 2.13) as the effective mass of isocurvature perturbations, we study the dispersion relations of the system of coupled perturbations Eq. 2.12 following [211–213]. We specialize to two fields and write the equations in terms of cosmic time t instead of efolds

$$\partial_t \left(\dot{\mathcal{R}} + \frac{2\Omega}{\sqrt{2\epsilon}} \mathcal{S} \right) + (3+\eta) H \left(\dot{\mathcal{R}} + \frac{2\Omega}{\sqrt{2\epsilon}} \mathcal{S} \right) + \frac{k^2}{a^2} \mathcal{R} = 0, \tag{2.14a}$$

$$\ddot{\mathcal{S}} + 3H\dot{\mathcal{S}} + \mu^2 \mathcal{S} + \frac{k^2}{a^2} \mathcal{S} = 2\sqrt{2\epsilon}\Omega \left(\dot{\mathcal{R}} + \frac{2\Omega}{\sqrt{2\epsilon}} \mathcal{S} \right). \tag{2.14b}$$

Let's write the solution as a sum of four normal modes

$$\begin{pmatrix} \mathcal{R} \\ \mathcal{S} \end{pmatrix} = \sum_{\omega} \begin{pmatrix} \mathcal{R}_\omega \\ \mathcal{S}_\omega \end{pmatrix} e^{-i \int dt\ \omega}. \tag{2.15}$$

Assuming the adiabatic condition $\dot{\omega}/\omega^2 \ll 1$, and neglecting both slow roll corrections and the rate of change of the turn rate $\dot{\Omega}$, we find the following linear system

$$\begin{pmatrix} -\omega^2 - 3Hi\omega + \frac{k^2}{a^2} & -i\omega \frac{2\Omega}{\sqrt{2\epsilon}} + 3H \frac{2\Omega}{\sqrt{2\epsilon}} \\ 2i\omega\sqrt{2\epsilon}\Omega & -\omega^2 - 3Hi\omega + \frac{k^2}{a^2} + \mu^2 - 4\Omega^2 \end{pmatrix} \begin{pmatrix} \mathcal{R}_\omega \\ \mathcal{S}_\omega \end{pmatrix} = \begin{pmatrix} 0 \\ 0 \end{pmatrix}. \tag{2.16}$$

We can most easily solve for the normal modes of the system of coupled damped harmonic oscillators by introducing the variable $\omega_0^2 \equiv \omega^2 + 3Hi\omega$, the eigenmodes of the undamped system. The solutions for ω_0^2 are given by

$$\omega_0^2 = \frac{k^2}{a^2} + \frac{1}{2}\mu^2 \pm \frac{1}{2}\sqrt{\mu^4 + 16\Omega^2 \frac{k^2}{a^2}}. \tag{2.17}$$

Therefore the four solutions are given by

$$\omega = \frac{-3Hi \pm \sqrt{-9H^2 + 4\omega_0^2}}{2}, \tag{2.18}$$

two normal modes for each solution of ω_0^2. Let's distinguish three cases:

- $\mu^2 \gg \frac{9}{4}H^2$. In this case we have heavy isocurvature perturbations which we can integrate out. Defining $c_s^2 \equiv 1 - \frac{4\Omega^2}{\mu^2}$, we have a few different regimes that the coupled oscillators will go through as the physical wavenumber $\frac{k}{a}$ redshifts during inflation.
  - If Ω is non-zero we can go to very small scales $4\left(1-c_s^2\right)\frac{k^2}{a^2} \gg \mu^2$ such that
  $$\omega_0^2 \approx \frac{k^2}{a^2} \pm \frac{2\Omega k}{a} \tag{2.19}$$
  The linear term is hardly ever important, because the inequality implies $\frac{k^2}{a^2} \gg \frac{\Omega^2}{(1-c_s^2)^2}$.
  - Then as soon as $4\left(1-c_s^2\right)\frac{k^2}{a^2} \ll \mu^2$ we find
  $$\omega_0^2 \approx \left(1 \pm \frac{4\Omega^2}{\mu^2}\right)\frac{k^2}{a^2} + \frac{1}{2}\mu^2\left(1 \pm 1\right). \tag{2.20}$$
  We can identify a dispersion relation ω_0^- corresponding to a massless excitation with reduced sound speed $(\omega_0^-)^2 = \frac{c_s^2 k^2}{a^2}$, and ω_0^+, corresponding to an excitation of mass μ. The massive excitation yields the following two normal modes
  $$\omega_\mu \approx -\frac{3Hi}{2} \pm \omega_0^+, \tag{2.21}$$
  i.e. two decaying and rapidly oscillating solutions of mass μ. Moreover, these solutions have $\mathcal{R}_\omega = 0$, if we neglect the Hubble friction. Therefore, this motivates us to interpret μ^2 as the effective mass of the isocurvature mass perturbations. The behavior of the massless excitation splits in two regimes:
    - On subhorizon scales $\frac{c_s^2 k^2}{a^2} \gg \frac{9}{4}H^2$ we get
    $$\omega \approx -\frac{3Hi}{2} \pm \frac{c_s^2 k^2}{a^2}. \tag{2.22}$$
    These are two underdamped harmonic oscillators
    - On superhorizon scales $\frac{c_s^2 k^2}{a^2} \ll \frac{9}{4}H^2$ we find
    $$\omega \approx -\frac{3Hi}{2}\left(1 \pm 1\right) \pm \frac{c_s^2 k^2}{a^2}\frac{i}{3H}, \tag{2.23}$$
    one overdamped harmonic oscillator and one solution that converges to a constant. These are exactly the two solutions we expect for $\mathcal{R}$. The interaction with the isocurvature perturbations is encoded in an effective reduced speed of sound c_s [201, 212, 214, 215].

- $\mu^2 \ll \frac{9}{4}H^2$. Assuming a non-zero value of $\Omega^2 < H^2$ we find that the solution for ω_0^2 splits in two regimes as before:
  - If we are at sufficiently small scales $16\Omega^2\frac{k^2}{a^2} \gg \mu^4$ we get

$$\omega_0^2 \approx \frac{k^2}{a^2} + \frac{1}{2}\mu^2 \pm \frac{2\Omega k}{a} \tag{2.24}$$

    The linear term is not important if we also ensure $\frac{k^2}{a^2} \gg 4\Omega^2$. Since $\mu^2 \ll H^2$ we can be either subhorizon or superhorizon:
    - Starting at subhorizon scales $\frac{k^2}{a^2} \gg \frac{9}{4}H^2 \gg \mu^2$ we find the solutions

$$\omega = -\frac{3Hi}{2} \pm \omega_0, \tag{2.25}$$

      corresponding to underdamped coupled harmonic oscillators of negligible mass.
    - On superhorizon scales $\frac{k^2}{a^2} \ll \frac{9}{4}H^2$ on the other hand we have

$$\omega = -\frac{3Hi}{2}(1 \pm 1) \pm \frac{i\omega_0^2}{3H}. \tag{2.26}$$

      We find two overdamped oscillators and two slowly decaying/growing solutions with exponential factor $-\frac{H}{3}\left(\frac{k^2}{a^2H^2} + \frac{1}{2}\frac{\mu^2}{H^2} \pm \frac{2\Omega k}{aH^2}\right)$. It depends on the values of μ and Ω which term is most important.
  - If $\mu \neq 0$, we can consider the regime $16\Omega^2\frac{k^2}{a^2} \ll \mu^4$. This leads to

$$\omega_0^2 \approx \left(1 \pm \frac{4\Omega^2}{\mu^2}\right)\frac{k^2}{a^2} + \frac{1}{2}\mu^2\left(1 \pm 1\right). \tag{2.27}$$

    On super horizon scales $\frac{k^2}{a^2} \ll \frac{9}{4}H^2$ we find the following eigenmodes

$$\omega = -\frac{3Hi}{2}(1 \pm 1) \pm \frac{i\omega_0^2}{3H}. \tag{2.28}$$

    In other words we find two overdamped oscillators, one slowly decaying solution with exponential factor $-\frac{H}{3}\frac{\mu^2}{H^2}$, and one solution that converges to a constant.

- $\mu^2 \sim H^2$. This is the typical quasi-single field regime [100]. Again, assuming that the turn rate is nonzero but $\Omega^2 < H^2$, we can distinguish two regimes.

– In case we have $\mu^4 \gg 16\Omega^2 \frac{k^2}{a^2}$, we find the same solution for ω_0 as in Eq. 2.27. On super-Hubble scales the four eigenmodes Eq. 2.18 contain a constant and decaying solution (when the $\pm$ is a $-$ in Eq. 2.27). The other solutions corresponding the the isocurvature mode are both decaying

$$\omega \approx -\frac{3Hi}{2} \pm \Delta\omega \tag{2.29}$$

where $\Delta\omega$ is imaginary if $\mu^2 \lesssim 9/4H^2$ and real if $\mu^2 \gtrsim 9/4H^2$. On sub-Hubble scales we find the same form as Eq. 2.29, but now $\Delta\omega = \omega_0$. This solution corresponds to four underdamped harmonic oscillators of mass zero and mass μ.

– For values $\mu^4 \ll 16\Omega^2 \frac{k^2}{a^2}$ we find the same ω_0^2 as in Eq. 2.24. This condition forces us to be on sub-Hubble scales. The dispersion relations are again given by Eq. 2.29 with $\omega \sim \frac{k^2}{a^2}$, corresponding to four undamped harmonic oscillators.

We conclude that on sub-Hubble scales the isocurvature perturbations behave like an underdamped harmonic oscillator of mass μ. On super-Hubble scales the Hubble friction takes over and the isocurvature perturbations freeze out ($\mu = 0$), slowly decay ($\mu^2/H^2 \ll 9/4$) or rapidly decay ($\mu^2/H^2 \gtrsim 1$).

This concludes our brief review of the kinematical description of linear perturbations in multi-field inflation. From now on we specialize to the two field scenario.

2.3 Phenomenology of Orbital Inflation

The results from § 2.2 equip us with all the necessary tools to study Orbital Inflation. We define Orbital Inflation as two-field inflation with a slowly varying entropy mass μ/H and a constant radius of curvature κ of the inflationary trajectory in field space (see Eq. 2.6). In this section we study how the predictions for the spectral tilt n_s and the tensor-to-scalar ratio r depend on μ and κ. For that purpose we restrict ourselves to a small entropy mass $0 \leq \mu^2/H^2 \leq 0.2$. In the regime where $\kappa/M_p \lesssim 10^2$ we find non-trivial results, and as far as we know the phenomenology of this regime has not been studied before, except for the limiting case $\mu^2/H^2 = 0$, see [138] and Chapter 3. For the limit of large entropy mass $\mu^2/H^2 \gg 1$ we refer the reader to Chapter 5. Let us emphasize, though, that in the next section, where we construct explicit models of Orbital Inflation, the entropy mass can take any value.

Using the results from § 2.2 we first derive an analytical approximation for the power spectrum of curvature perturbations based on the evolution of the coupled perturbations on super-Hubble scales. We complement this with a numerical computation [216–219] when we present the results in Figure 2.2. To address the validity of the perturbative numerical computation and our simple analytical estimate we need the quadratic action of perturbations. Moreover, we also need it to have the right normalization of the fields when we quantize the theory. For two-field inflation, in efolds, it is given by [138]

$$S^{(2)} = \frac{1}{2}\int dN d^3x a^3 M_p^2 H \left[2\epsilon\left(\mathcal{R}' - \frac{2M_p}{\kappa}\mathcal{S}\right)^2 + (\mathcal{S}')^2 - \frac{\mu^2}{H^2}\mathcal{S}^2 + \ldots\right] \tag{2.30}$$

The ellipses denote the gradient terms $-(\partial_i\mathcal{S})^2/H^2 - 2\epsilon(\partial_i\mathcal{R})^2/H^2$. The linearized system of coupled perturbations Eq. 2.12 for two fields reads

$$(\partial_N + 3 - \epsilon - \eta)\left(\mathcal{R}' - \frac{2M_p}{\kappa}\mathcal{S}\right) + \frac{k^2}{a^2H^2}\mathcal{R} = 0, \tag{2.31a}$$

$$(\partial_N + 3 - \epsilon)\,\mathcal{S}' + \left(\frac{\mu^2}{H^2} + \frac{k^2}{a^2H^2}\right)\mathcal{S} = -\frac{4\epsilon M_p}{\kappa}\left(\mathcal{R}' - \frac{2M_p}{\kappa}\mathcal{S}\right). \tag{2.31b}$$

Notice that we have rewritten the turn rate Ω in terms of the radius of curvature κ, defined in Eq. 2.6. On super-Hubble scales $k^2 \ll a^2H^2$, the equations simplify considerably. The equation of motion for $\mathcal{R}$ has the solution

$$\mathcal{R}' - \frac{2M_p}{\kappa}\mathcal{S} = 0 + \text{decaying part}. \tag{2.32}$$

Meanwhile, neglecting the decaying part on the right hand side of Eq. 2.31b, the equation for $\mathcal{S}$ reduces to

$$\mathcal{S}'' + (3-\epsilon)\mathcal{S}' + \frac{\mu^2}{H^2}\mathcal{S} = 0. \tag{2.33}$$

For approximately constant $0 < \mu^2/H^2 \ll 9/4$ and $\epsilon \ll 1$, this equation describes an overdamped oscillator with solution

$$\mathcal{S}(N) \approx \mathcal{S}_0 e^{-\frac{N-N_0}{3}\frac{\mu^2}{H^2}} + \text{decaying part}. \tag{2.34}$$

The isocurvature perturbations in turn source the curvature perturbations, through Eq. 2.32 . Integrating this equation gives the superhorizon solution for $\mathcal{R}$:

$$\mathcal{R}(N) \approx \mathcal{R}_0 + \mathcal{S}_0\frac{6M_pH^2}{\mu^2\kappa}\left(1 - \exp\left(-\frac{N}{3}\frac{\mu^2}{H^2}\right)\right). \tag{2.35}$$

Here we made use of the fact that κ is constant. In the limit that $\mu^2/H^2 = 0$, the isocurvature perturbation freezes out at horizon crossing, conform Eq. 2.34.

In this case the second term in Eq. 2.35 becomes proportional to ΔN, which is in agreement with the expansion of this term for small μ^2/H^2. In the quantum analysis of two-field inflation [198] there are two uncorrelated contributions to $\hat{\mathcal{R}}$. The first contribution is sourced by initial curvature perturbations where $\mathcal{S}_0 = 0$. This corresponds to the constant mode $\mathcal{R}_0$ that freezes out on super-Hubble scales. The second contribution is sourced by initial isocurvature perturbations, and corresponds to the second solution proportional to $\mathcal{S}_0$. Using the typical amplitude of quantum perturbations at horizon crossing $\mathcal{S}_0 \sim \sqrt{2\epsilon}\mathcal{R}_0 \sim \frac{H}{2\pi}$, the power spectrum of curvature perturbations is given by[3]

$$P_{\mathcal{R}} \approx \frac{H^2}{8\pi^2\epsilon M_p^2}\left(1 + 2\epsilon\left(\frac{6M_pH^2}{\mu^2\kappa}\right)^2\left(1 - \exp\left(-\frac{\Delta N}{3}\frac{\mu^2}{H^2}\right)\right)^2\right) . \tag{2.37}$$

Here all variables are understood to be evaluated at horizon crossing, and ΔN denotes the number of efolds counted from when the observable modes cross the horizon until the end of inflation. In the limit of small entropy mass μ^2/H^2, we can expand the exponential in Eq. 2.37 to find that this terms scales as $\Delta N^2/\kappa^2$. To get an improved analytical result, one can perform a full in-in computation similar to what is done in [138]. We checked our simple analytical estimate numerically by means of the exact models described in § 2.4.2, using the Python code developed by [218, 219], and found that it works well for $\kappa^2/M_p^2 \geq 1$. We plot the results for n_s and r in Figure 2.2. The analytical results are obtained by using

$$n_s = \frac{\partial \ln P_{\mathcal{R}}}{\partial N}, \quad r = \frac{2H^2}{\pi^2 M_p^2}\frac{1}{P_{\mathcal{R}}}, \quad \epsilon = \frac{p}{2\Delta N + p} . \tag{2.38}$$

The numerical results are computed using the following potential and kinetic term

$$V(\theta, \rho) = 3M_p^4\left(\theta^2 + \frac{2M_p^2}{3f(\rho)}\right)\left(1 + \frac{\lambda}{12}\frac{(\rho - \rho_0)^2}{M_p^2}\right)^2 , \tag{2.39a}$$

$$2K = f(\rho)(\partial\theta)^2 + (\partial\rho)^2 \quad \text{with} \quad f(\rho) = e^{2\rho/R_0} . \tag{2.39b}$$

[3] As a cross-check we compare the obtained power spectrum with that of quasi-single field inflation [100]. Matching with the numerical function $\mathcal{C}(\nu)$ defined in Eq. (3.8) of [100], we find

$$\mathcal{C}(\nu) = \frac{9}{2}\frac{1}{\left(\frac{9}{4} - \nu^2\right)^2}\left(1 - \exp\left(-\frac{\Delta N}{3}\left(\frac{9}{4} - \nu^2\right)\right)\right)^2 . \tag{2.36}$$

This seems to agree reasonably well if we take $\Delta N \sim 50 - 60$, even for μ^2/H^2 close to 9/4. When $\kappa^2/M_p^2 \lesssim 10^2$ We don't find the same prediction for n_s as in Eq. (3.11) of [100], because the second term in Eq. 2.37 becomes important, and we have to take into account the ΔN-dependence of $C(\nu)$.

The field metric is hyperbolic with curvature $\mathbb{R} = -\frac{2}{R_0^2}$. As explained in § 2.4.2 this model admits Orbital Inflation with $\kappa^2 = R_0^2$ and $\mu^2/H^2 = \lambda\left(1 - \frac{1}{3}\epsilon\right)$.

In Figure 2.2 we vary κ^2/M_p^2 between 1 and 10^5. The lower bound comes from the validity of the perturbative approach we implicitly assumed. The numerical code [218] is performing a tree level in-in computation, and higher order tree level (and loop) corrections should be small compared to the leading result. Our simple analytical result captures the super-Hubble evolution of $\mathcal{R}$, and therefore provides an estimate of the leading order tree level computation. Using Eq. 2.30 we can estimate that $\alpha \sim \sqrt{8\epsilon}\frac{M_p}{\kappa}$ is the perturbation parameter that measures the relative size of the higher order tree level corrections compared to the leading tree level computation[4]. Therefore, we need to ensure that $\alpha \ll 1$, which is why we take $\kappa/M_p \geq 1$. At the same time we should be careful that quantum perturbations remain much smaller than the radius of curvature $\delta\rho \ll \kappa$. In particular, we should be careful in the limit that the isocurvature perturbations are very light $\mu^2/H^2 \ll 1$. Fortunately, this is the case. If we consider small values of κ, such that the second term in Eq. 2.37 dominates, we get $P_{\mathcal{R}} \sim \frac{H^2}{\kappa^2}$. Since the amplitude of the power spectrum is fixed by observations $A_{\mathcal{R}} \sim 10^{-9}$, this implies that the typical size of quantum fluctuations gets suppressed if we decrease κ. We find $\delta\rho^2 \sim H^2 \sim \kappa^2 A_{\mathcal{R}} \ll \kappa^2$, so we are always fine.

From Figure 2.2 we see that the observable predictions are already significantly modified for $\kappa^2/M_p^2 \lesssim 10^3$ (for $\mu^2/H^2 = 0$) or $\kappa^2/M_p^2 \lesssim 10^2$ (for $\mu^2/H^2 \approx 0.2$). Interestingly, the entropy mass μ^2/H^2 dictates how the inflationary predictions fan out in the (n_s, r) plane. In particular, the various entropy masses predict a different change in n_s. It would be very interesting to see if this effect may allow us to *distinguish* between the various entropy masses. This requires a complementary analysis of the bispectrum. For these models we expect to find local primordial non-Gaussianities, because the super-Hubble evolution of $\mathcal{R}$ is the dominant contribution to its final amplitude. Therefore, in future work we plan to assess the amplitude and the scale-dependence of the bispectrum in the squeezed configuration. In particular, we would like to understand its dependence on the kinematical and geometrical parameters of multi-field inflation. This should give us more insight what to expect from the simplest modifications to the single field inflationary scenario.

[4] In the in-in computation the sourcing of $\mathcal{R}$ by $\mathcal{S}$ is captured by the interaction term $S^{(2)}_{\rm int} = \int d\tau d^3x a^3 4\epsilon \frac{M_p^3 H}{\kappa}(\partial_\tau \mathcal{R})\mathcal{S}$ (using Eq. 2.30 written in terms of conformal time $d\tau = dN/aH$.) Rewriting this in canonical variables $u \equiv \sqrt{2\epsilon} a M_p \mathcal{R}$ and $v \equiv a M_p \mathcal{S}$ we get $S^{(2)}_{\rm int} \sim \int d\ln\tau d^3x\ \alpha(\partial_\tau u)v$, with $\alpha = \sqrt{8\epsilon}\frac{M_p}{\kappa}$.

Finally, we should also estimate the relative amplitude of isocurvature perturbations compared to the amplitude of curvature perturbations. How they are related to the late-time non-adiabatic perturbations depends on the mechanism of reheating, but we may still want to ensure that they are suppressed at the end of inflation. From Eq. 2.34 we see that the isocurvature perturbations decay on super-Hubble scales if $\mu^2/H^2 \gtrsim 3/\Delta N$, so we can assume that isocurvature perturbations with entropy masses of $\mu^2/H^2 \gtrsim 0.06$ have decayed by the end of inflation. However, for $\mu^2/H^2 \lesssim 0.06$, we should be more careful. The ratio between curvature and isocurvature perturbations is given by

$$\beta_{\text{iso}} \equiv \frac{P_{\mathcal{S}}}{2\epsilon P_{\mathcal{R}}} \approx \frac{1}{1 + 8\epsilon \frac{M_p^2 \Delta N^2}{\kappa^2}} \,. \tag{2.40}$$

To arrive at this result, we expanded the exponential in Eq. 2.34. Therefore, our results are reliable in the regime

$$1 \gg 8\epsilon \frac{M_p^2}{\kappa^2} \gg \frac{1}{\Delta N^2} \quad (\text{or } \mu^2/H^2 \gtrsim 0.1) \tag{2.41}$$

Fortunately, this is contained in the regime where we find non-trivial results.

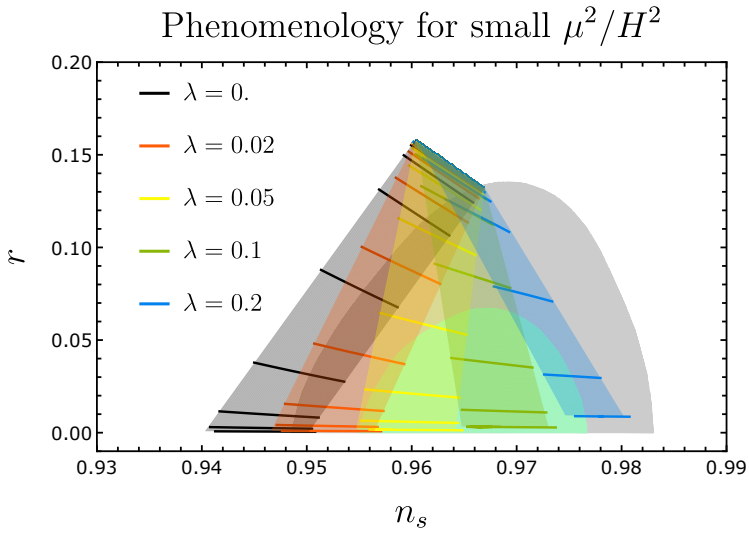

Figuur 2.2: This figure shows the predictions of (n_s, r) for the model given in Eq. 2.39 using the numerical code [218, 219]. The entropy mass takes five different values, as indicated in the legend, with $\mu^2/H^2 = \lambda\left(1 - \frac{1}{3}\epsilon\right) \approx \lambda$. The solid lines correspond to $R_0^2/M_p^2 \in \{1, 4, 4^2, \ldots, 4^8\}$ from bottom to top, and we let $\Delta N \in [50, 60]$. On top of that we plot our analytical results (coloured shaded regions) using Eq. 2.38, where vary κ^2/M_p^2 between 1 and 10^5. Furthermore, on the background we plotted the 1σ and 2σ confidence contours from *Planck* [115].

2.4 Exact models of Orbital Inflation

In this section we derive exact models of Orbital Inflation. For this we first generalize the Hamilton-Jacobi formalism [74, 75, 77, 78] to two-field inflation in § 2.4.1, which we use in § 2.4.2 to perform an explicit construction.

2.4.1 Hamilton-Jacobi for two-field inflation

We generalize the Hamilton-Jacobi formalism to two-field inflation, such that we can locally reconstruct the potential similar to the single field case described in § 1.2.3. The first step is to replace the time coordinate with the proper field distance φ along the inflationary trajectory

$$\varphi \equiv \int dt \, \sqrt{G_{ab} \frac{d\phi^a}{dt} \frac{d\phi^b}{dt}} \, . \tag{2.42}$$

Given the Hubble slow roll parameters, we know that we can reconstruct the potential *on the inflationary trajectory*, following § 1.2.3. However, in the two-field case we would like to reconstruct the potential in the neighborhood of the inflationary trajectory as well. In fact, from Eq. 2.8 we know that the gradient

of the potential in the orthogonal direction should be such that it counterbalances the centrifugal force. This provides an additional constraint in the two-field scenario. Generically, H is a function of the normal field coordinates σ_i as well. Therefore we might as well parameterize the Hubble parameter in terms of any set of field coordinates $H = H(\phi^a)$. This is fine as long as all coordinates are stricly increasing or decreasing on the inflationary trajectory.

Similarly to the single field case we have a solution for every initial value $H(\phi_0^a)$, however this cannot cover all possible initial data. In the case of two-field inflation we therefore need an additional function $F(\phi^a)$ to fully specify the system. Indeed, using the second Friedmann equation Eq. 2.4c we find

$$\dot{H} = \dot{\phi}^a H_a = -\frac{\dot{\phi}^a \dot{\phi}^b G_{ab}}{2M_p^2} \quad \longrightarrow \quad H_a = -\frac{G_{ab}\dot{\phi}^b}{2M_p^2} + F(\phi^b) N_a \ . \tag{2.43}$$

Note that we have the freedom to add to H_a any contribution proportional to the normal vector to the trajectory, because it is projected out when contracting with $\dot{\phi}^a$ to get $\dot{H}$. Using Eq. 2.43, we rewrite the first Friedmann equation as the multi-field Hamilton-Jacobi equation

$$3H^2 M_p^2 = V + 2M_p^4 \left(H^a H_a - F^2 \right) . \tag{2.44}$$

Notice that we need both H and F to fully determine the system. This equation contains the same information as the tangent projection of the field equations. To see this we write Eq. 2.44 as

$$3H^2 M_p^2 = V + 2M_p^4 H_\varphi^2 \quad \text{with} \quad H_\varphi = H_T = -\frac{\dot{\varphi}}{2M_p^2} \tag{2.45}$$

and take a derivative with respect to φ to find Eq. 2.8a. In addition we have to obey the normal projection of the field equations Eq. 2.8b, which provides a constraint on F. We compute $D_t T^a$ using $T^a = -\frac{2M_p^2}{\dot{\varphi}} \left(H^a - F N^a \right)$. Moreover V_N can be computed using Eq. 2.44. Together they lead to the constraint equation

$$3HF - 2M_p^2 H_T F_T + 2F \left(F_N - H_{NN} \right) = 0 \ . \tag{2.46}$$

In particular, $F = 0$ gives a solution compatible with the constraint equation. However, there are also solutions that have a non-trivial F.

At this point we would like to stress that we intend to apply the Hamilton-Jacobi formalism to reconstruct the potential in the neighborhood of a given inflationary trajectory only. Therefore, we only need to solve for Eq. 2.44 and Eq. 2.46 *on the trajectory*. These equations restrict the normal projection of

the gradient of the potential, but other than that they leave the potential free. For this local reconstruction it might be convenient to pick the natural kinematical field coordinates. This implies that each normal vector is parallel transported along its normal direction, i.e. $N_i^a \nabla_a N_i^b = 0$. In the two-field case we therefore have $H_{NN} \equiv N^a N^b \nabla_a \nabla_b H = N^a \nabla_a F \equiv F_N$ and the constraint equation further simplifies to

$$3HF - 2M_p^2 H_\varphi F_\varphi = 0 \,. \tag{2.47}$$

This restricts the form of F only at $\sigma = \sigma_0$, i.e. on the trajectory. We will next see that this allows us to construct inflationary models with any isocurvature mass.

2.4.2 Orbital inflation

We are now ready to construct inflationary potentials with constant κ and (almost) constant μ^2/H^2, using Eq. 2.44 and Eq. 2.47. A constant radius of curvature can be achieved by considering an inflationary trajectory that proceeds along an isometry direction of the field metric that is *not* a geodesic. This is the key characteristic of the exact models of Orbital Inflation. And in this sense it is an attempt of realizing spontaneously symmetry probing [196] in inflation. The existence of an isometry implies that we are free to choose our field coordinates (θ, ρ), such that the field metric G_{ab} does not depend on θ. Moreover, we have also the freedom to put $G_{\theta\rho}$ to zero[5]. Furthermore, we denote $f(\rho) = G_{\theta\theta}$.

We would like to reconstruct the potential that admits Orbital Inflation, that is, solutions of the form

$$\dot\rho = 0, \quad \dot\theta < 0. \tag{2.48}$$

The sign of $\dot\theta$ is our choice of convention, also we take $\theta > 0$ on the inflationary trajectory. This means we can replace $\varphi \to \sqrt{f}\theta$ and $H_\varphi \to \frac{1}{\sqrt{f}} H_\theta$. Moreover, the relevant kinematical and geometrical inflationary background quantities simplify to

$$T^a = \frac{1}{\sqrt{f}}(-1,\ 0) \quad \text{and} \quad N^a = (0, 1), \tag{2.49a}$$

$$\dot\theta = -2M_p^2 \frac{H_\theta}{f}, \quad \epsilon = \frac{2M_p^2 H_\theta^2}{f H^2}, \quad \kappa = \frac{2f}{\partial_\rho f}, \quad \mathbb{R} = \frac{2}{\kappa^2} - \frac{f_{\rho\rho}}{f}. \tag{2.49b}$$

[5] If $G_{\theta\rho} \neq 0$, define $\tilde\theta = \theta + \int d\rho\, \frac{G_{\theta\rho}(\rho)}{G_{\theta\theta}(\rho)}$ such that $\tilde G_{\tilde\theta\rho} = 0$.

Here $f = f(\rho)$ and $H = H(\theta, \rho)$. On the desired inflationary trajectory the radial coordinate takes a constant value ρ_0. Therefore, we expand $H(\rho, \theta)$ around $\rho = \rho_0$:

$$H(\rho,\theta) = M_p \left(W(\theta) + X(\theta)\frac{\rho-\rho_0}{M_p} + Y(\theta)\frac{(\rho-\rho_0)^2}{M_p^2} + \dots \right) . \tag{2.50}$$

Moreover, we take $F(\rho, theta) = \partial_\rho H(\rho, \theta)$. We insert this into the constraint equation Eq. 2.46 to identify the restrictions on $X(\theta)$. First of all, on the desired inflationary trajectory we have $F = H_\rho$ and $H_{\rho\rho} = F_\rho$, which allows us to use Eq. 2.47. Moreover, we express tangent derivatives in terms of derivatives with respect to θ. The constraint equation simplifies to

$$3W(\theta)X(\theta) - \frac{2W_\theta(\theta)X_\theta(\theta)M_p^2}{f(\rho_0)} = 0 . \tag{2.51}$$

An obvious solution is given by $X(\theta) = 0$, which we will assume for simplicity. Next, we compute the effective mass of isocurvature perturbations. For the orbital inflationary trajectory we have $\mu^2 = V_{\rho\rho} + \epsilon M_p^2 H^2 \left(\mathbb{R} + \frac{6}{\kappa^2}\right)$, which can be written as

$$\mu^2 = 12M_p^2 Y(\theta)W(\theta) - \frac{8M_p^4}{f(\rho_0)} Y_\theta(\theta)W_\theta(\theta) . \tag{2.52}$$

Therefore, we can construct a potential with any isocurvature mass we like. For instance, specializing to $Y(\theta) = \frac{1}{12}\lambda W(\theta)$ yields

$$\left.\frac{\mu^2}{H^2}\right|_{\rho=\rho_0} = \lambda \left(1 - \frac{2M_p^2}{3f(\rho_0)} \frac{W_\theta^2(\theta)}{W^2(\theta)} \right) . \tag{2.53}$$

Notice that the second term in Eq. 2.53 is proportional to the slow roll parameter ϵ on the trajectory, using Eq. 2.49. Therefore, well within the slow-roll regime we approximately get $\frac{\mu^2}{H^2} \approx \lambda$.

It should be clear that if one continues in this fashion, combinations of the higher order derivatives of the potential can be tuned as well. For instance, this technique may be used to contruct explicit quasi-single-field models of inflation with large $V_{\rho\rho\rho}$ [100]. Moreover, there are many more ways to arrive at a constant entropy mass. For now we put the higher order corrections to H and F to zero, and use Eq. 2.44 to find

$$V(\theta,\rho) = 3M_p^4 \left(W^2(\theta) + \frac{2M_p^2 W_\theta^2(\theta)}{3f(\rho)} \right) \left(1 + \frac{\lambda}{12}\frac{(\rho-\rho_0)^2}{M_p^2} \right)^2 , \tag{2.54}$$

which constitutes a realization of Orbital Inflation. Finally, using the results from § 1.2.3, we may choose $W(\theta) = \theta^p$ such that ϵ is given by

$$\epsilon = \frac{p}{2\Delta N + p}, \tag{2.55}$$

where ΔN denotes the number of efolds before the end of inflation where the observable modes cross the horizon. We used this potential with $p = 1$ in the numerical/analytical computations presented in Figure 2.2.

Finally, we would like to point out an interesting limit. Notice that we can locally achieve a zero entropy mass μ by choosing $Y(\theta) = 0$. If we demand Orbital Inflation at *any* radius ρ_0 with $\mu = 0$, this forces H to be a function of θ only. Therefore the masslessness of radial perturbations corresponds to a radial shift symmetry in H rather than in the resulting potential. We study this particular limit in Chapter 3.

2.5 Summary

In two-field inflation there are only a few kinematical and geometrical parameters that determine the evolution of linear perturbations. These are the *radius of curvature* of the inflationary trajectory in field space, the *entropy mass* (the mass of the isocurvature perturbations) and the Hubble slow-roll parameters. This motivates us to introduce Orbital Inflation, in which the radius of curvature is constant, and the remaining parameters are slowly varying. This is one of the simplest two-field extensions to single field inflation.

In § 2.3 we discussed the phenomenology of Orbital Inflation. In particular we focus on the regime of small entropy mass $\mu^2/H^2 \leq 0.2$ and we found that the predictions are substantially modified already for $\kappa^2/M_p^2 \lesssim 10^2$. Furthermore, in § 2.4 we showed how to explicitly construct exact models of Orbital Inflation. The key characteristic of these models is that inflation proceeds along an isometry direction of the field metric. We used a generalization of the Hamilton-Jacobi formalism to find the potential *locally* around the inflationary trajectory. Finally, we saw that an interesting limiting case is to have a vanishing entropy mass. This is reflected by a shift symmetry in the Hubble parameter rather than in the resulting potential. We investigate this particular case in Chapter 3.

For convenience of the reader, we collect the relevant formulas and elements that describe the two-field models we have reconstructed in § 2.4. The

procedure is more general, and can be used to reconstruct other multi-field models of inflation as well

- We specialized to a two-field model with two scalar fields θ and ρ described by the following action

$$S = \frac{1}{2}\int d^4x\sqrt{-g}\left[M_p^2 R - f(\rho)\partial_\mu\theta\partial^\mu\theta + \partial_\mu\rho\partial^\mu\rho - 2V(\theta,\rho)\right] \ . \quad (2.56)$$

  with R the Ricci scalar of spacetime. The scalar kinetic term has an isometry in the θ direction.

- In order to achieve a constant radius of curvature, we force inflation to proceed exactly in the θ direction. This puts a restriction on the form of $H(\rho,\theta)$, namely that it has to be independent of θ on the trajectory $\rho = \rho_0$.

- Next, we compute the entropy mass in terms of $H(\rho,\theta)$ expanded around $\rho = \rho_0$. We took into account that the entropy mass, defined in Eq. 2.13, receives geometrical and kinematical corrections as well. This allowed us to reconstruct the following potential, which admits an approximately constant entropy mass $\mu^2/H^2 \approx \lambda$ up to slow-roll corrections

$$V = 3M_p^4\left(W^2(\theta) + \frac{2M_p^2 W_\theta^2(\theta)}{3f(\rho)}\right)\left(1 + \frac{\lambda}{12}\frac{(\rho-\rho_0)^2}{M_p^2} + \dots\right)^2 , \quad (2.57)$$

  The ellipses denote higher order terms in the expansion around $\rho = \rho_0$ we left unspecified. They determine higher order derivatives of the potential, such as $V_{\rho\rho\rho}$.